Appendix 1. AMSRIce03 Field Report

AMSR-Ice03: Field Validation Campaign for AMSR-E Polar Ocean Products Beaufort and Chukchi Seas, March 2003 Field Program Report

Matthew Sturm[1], James Maslanik[2], Don Perovich[3], Julienne Stroeve[4], Jackie Richter-Menge[3], Don Cavaliri[5], Thorsten Markus[5], Jon Holmgren[1], John Heinrichs[6], Ken Tape[7]

[1]U.S. Army Cold Regions Research & Engineering Laboratory-Alaska, Fairbanks, AK
[2]Colorado University, Engineering & Aerospace, Boulder, CO
[3]U.S. Army Cold Regions Research & Engineering Laboratory, Hanover, NH
[4]CIRES, University of Colorado, Boulder, CO
[5]NASA-Goddard Space Flight Center, Greenbelt, MD
[6]Ft. Wayne State College,
[7]Geophysical Institute, University of Alaska-Fairbanks, Fairbanks, AK

Executive Summary

In March, 2003, a field validation campaign was conducted on the sea ice near Barrow, Alaska. The goal of this campaign was to produce an extensive data of sea ice and snow properties during the same period that the area was overflown by a NASA P-3 aircraft armed with multiple remote sensing instruments, including one that mimics the performance of the AMSR-E satellite. Field, airborne, and satellite data were to be compared in order to proof and improve existing algorithms for sea ice retrieval of the AMSR-E satellite. In addition, the sea ice and snow data were to be used to investigate the nature of snow and ice heterogeneity.

Twelve people participated in the field campaign, which lasted from March 3rd until March 23rd. There were two field locations: the coastal sea ice near Barrow, Alaska, and ice pack at a U.S. Navy camp several hundred kilometers north of the Alaskan coast. On 20 km of traverse lines we collected thousands of snow depth, ice thickness and snow and ice temperature measurements. Additional information collected included extensive snow and ice characterizations, continuous profiles of brightness (Tb) and surface temperature, and more than 100 low-altitude aerial photographs.

With respect to spatial heterogeneity, three types of snow and ice systems were measured: 1) first year ice (FYI) with little deformation (at Elson Lagoon), 2) FYI with various amounts of deformation (minimal to extreme)(on the ice of the Chukchi and Beaufort seas near Barrow), and 3) Mixed FYI and multi-year ice (MYI) (Navy camp) with various degrees of deformation. Relatively similar degrees of snow and ice heterogeneity exist across all three types of snow/ice systems despite differences in ice properties and roughness, with striking similarities between FYI ice of the Beaufort Sea just off Barrow and ice of the Beaufort Sea hundreds of kilometers offshore.

1. Introduction

The AMSR-E satellite is expected to produce data sets from which critical changes in the cryosphere, like the extent of sea ice, can be derived. These will form the basis of time series that will allow us to assess climate trends and their impact. A critical step in ensuring that these time series are accurate and useful is to calibrate and validate the new sensors. Here we describe a field validation/calibration campaign that took place in March, 2003 on the sea ice near and offshore from Barrow, Alaska. The field campaign was a combined effort from many institutions, including the U.S. Army Cold Regions Research and Engineering Laboratory, Colorado University, and NASA Goddard Space Flight Center.

Here we describe details of the field component of the campaign. Twelve people worked on the sea ice near Barrow, Alaska, and offshore at a Navy Ice Camp, for three weeks in March of 2003. The goal of the field work was to develop a "legacy" data set against which remote sensing products from aircraft and satellite could be compared. We had three objectives with respect to the data:

- Ensure that field data and aircraft data were co-located (this as proven surprisingly hard to achieve in previous campaigns).
- Collect as spatially-extensive a data set as possible in order to minimize issues related to comparing point measurements to remote sensing (areal measurements).
- Use field mapping and aerial photography to further reduce issues related to mismatch in spatial extent when comparing field and remote measurements.
- Use the extensive field measurements to begin to investigate the nature of the spatial heterogeneity of near-shore and off shore arctic sea ice.

The reader will come to his/her own conclusions was to whether we accomplished these objectives, but is the opinion of the authors that we achieved items 1 through 3, and the prospects for answering fundamental questions related to item 4 look promising.

This report is organized in two sections. The first (Navy Ice Camp) reports on the data collected on the ice of the Beaufort Sea several hundred kilometers north of Barrow. The second (Barrow) reports on the data collected on the ice in the vicinity of Barrow, Alaska. Both sections include discussion of the heterogeneity of the snow and sea ice. The second section includes comparisons of the heterogeneity at Barrow and the Navy Ice Camp. The report ends with some preliminary conclusions and a list of on-going a and future work.

2. The Navy Ice Camp

2.1 Location

We worked at the Navy Ice Camp from 18 to 22 March. The P-3 flew over the camp on 19 March. Ground measurements consisted of a main measurement line 4.47 km long (orientation 14°T), and five (5) cross lines each 0.1 km long (Fig. 1). Appendix 1 provides the GPS coordinates for the main line and can be used to convert distance along the line to latitude/longitude. The GPS readings were taken March 19th during a 3 hour period that bracketed the aircraft overflight.

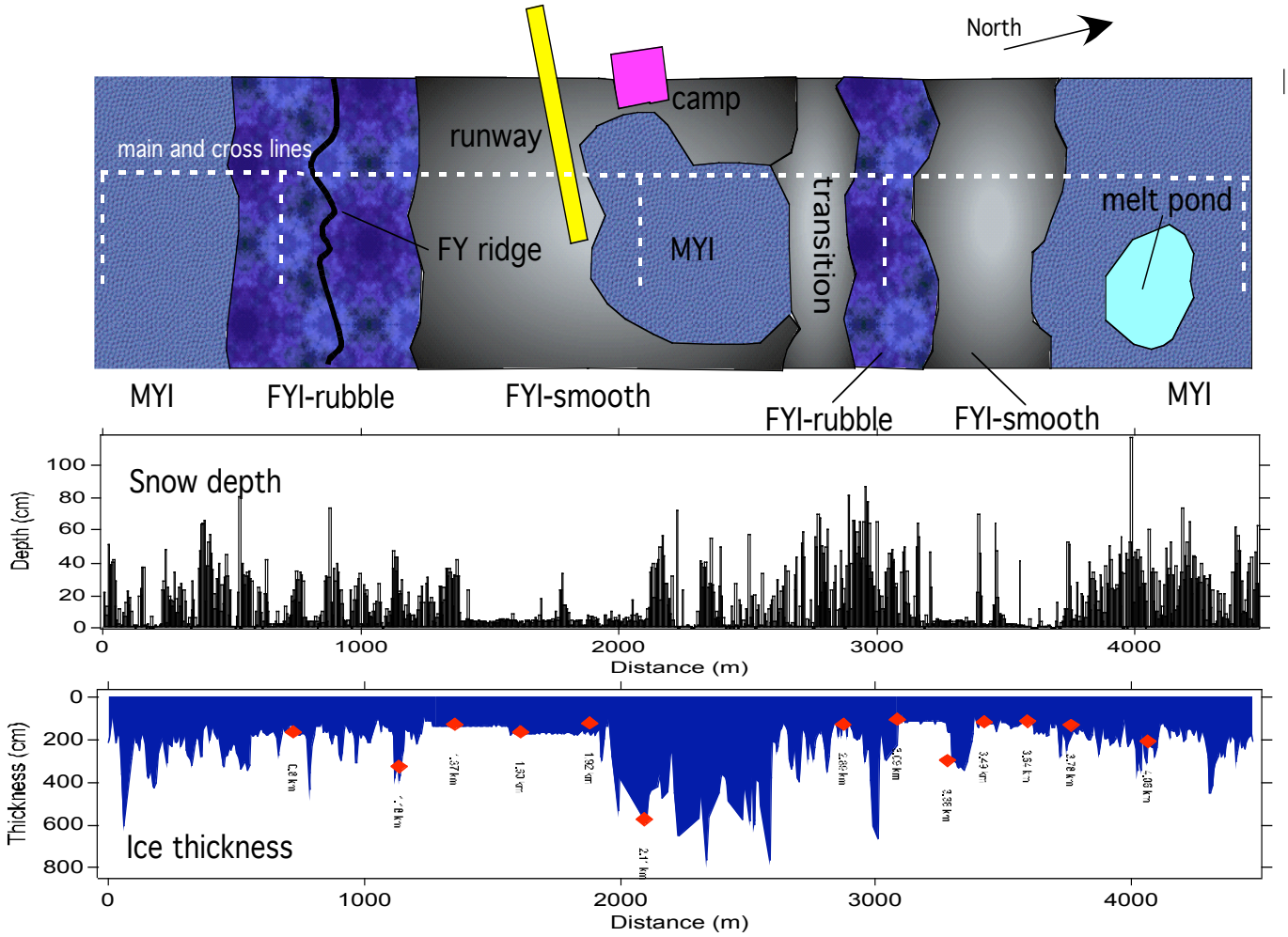

Figure 1: The Navy Ice Camp and environs with a general map of ice types and the related snow and ice thickness measurements from the main line. The approximate locations of the main and cross measurement lines are shown with white dashed lines in the top panel. The red diamonds are ice thicknesses from drill holes.

The closest the aircraft flight lines came to the main measurement line at the Ice Camp was 1 km (Fig. 2). This "nearest approach" took place during a southbound pass, the 11th pass of the mission. The on-ice data were to the right of the aircraft, so at an altitude of about 1200m, a side-look nadir angle of about 45° would produced data coincident with the on-ice measurements.

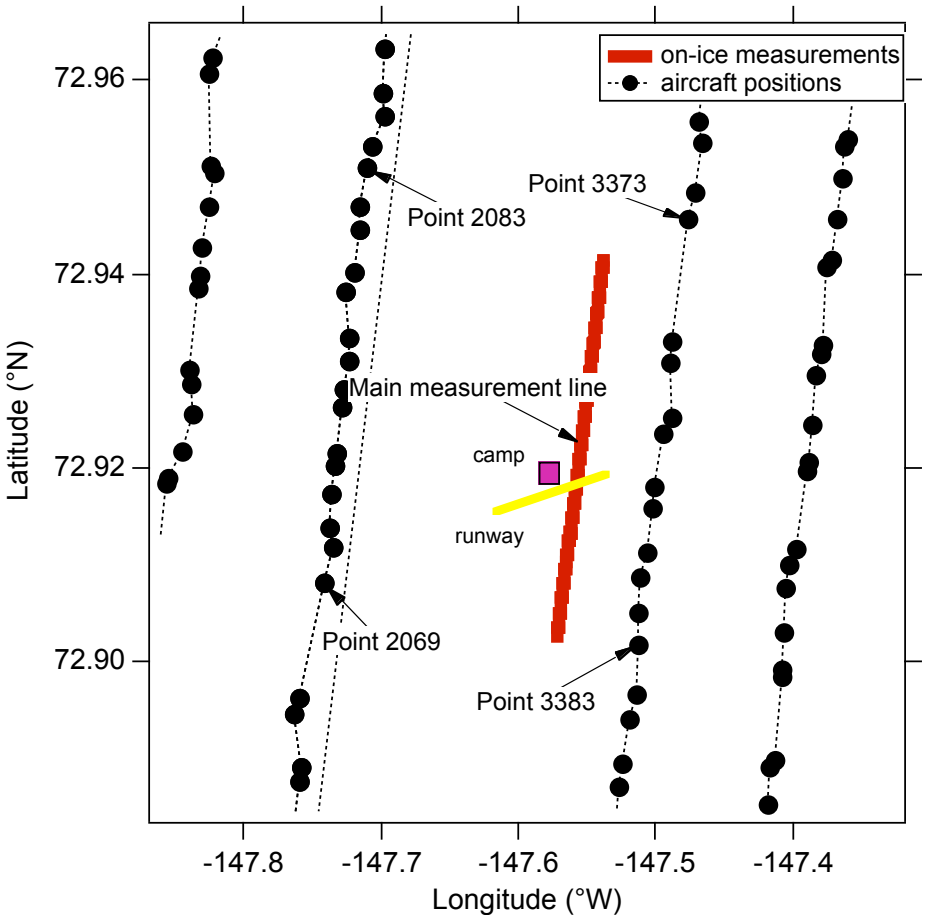

Figure 2: Location of aircraft positions and ground measurements for March 19th.

The data collected at the Navy Ice Camp consisted of:

- Snow depth
- Snow stratigraphy, density and grain size
- Ice thickness (from drill holes and using an EM-31)
- Ice cores for physical properties.
- Snow and ice temperature
- Snow "skin" temperature.

2. 2 Results-Navy Ice Camp

2.2.1 Snow

There was a wide range of sea ice types at the Ice Camp. As Figure 1 suggests, with the exception of nilas and other very young forms of ice, all types of first year (FYI) and multiyear (MYI) were present along the main measurement line. Results across all types of ice indicate a mean snow depth of 16.7 cm (n =901), with a standard deviation of 17.5 cm (Fig. 3). More than 25% of all measurements were in snow less than 5 cm deep, a fact consistent with the extensive areas of bare ice that were observed.

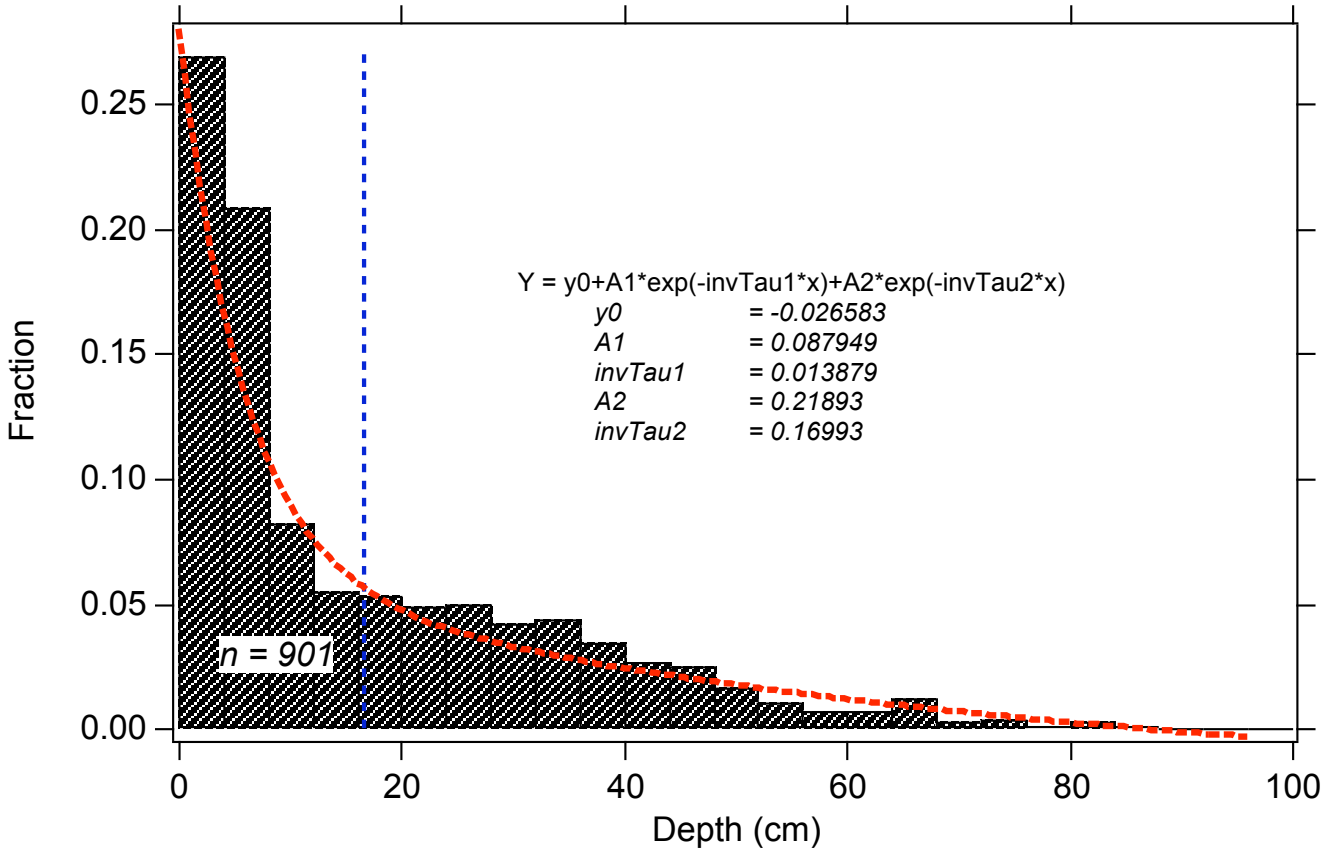

Figure 3: Histogram of snow depth for all types of ice on the main measurement line at the Navy Ice Camp. The mean (16. 7 cm) is indicated by the vertical dashed line. A double exponential curve has been fit to the distribution (thick dashed red line).

We know the distribution shown in Figure 3 is a composite of snow depths from a number of types of ice, so we have examined these individually to see if they differed significantly. In Figure 4, the depth profile for the main line is shown divided into segments based on our field mapping of ice types (Fig. 1). For each segment we have tabulated depth statistics in Table 1 (see also Appendix 2). We have added to these the results of the cross lines, each of which was 100 m long and consisted of 201 depth

measurements taken on an equal spacing. Summary statistics for each segment and cross line appear in Table 1.

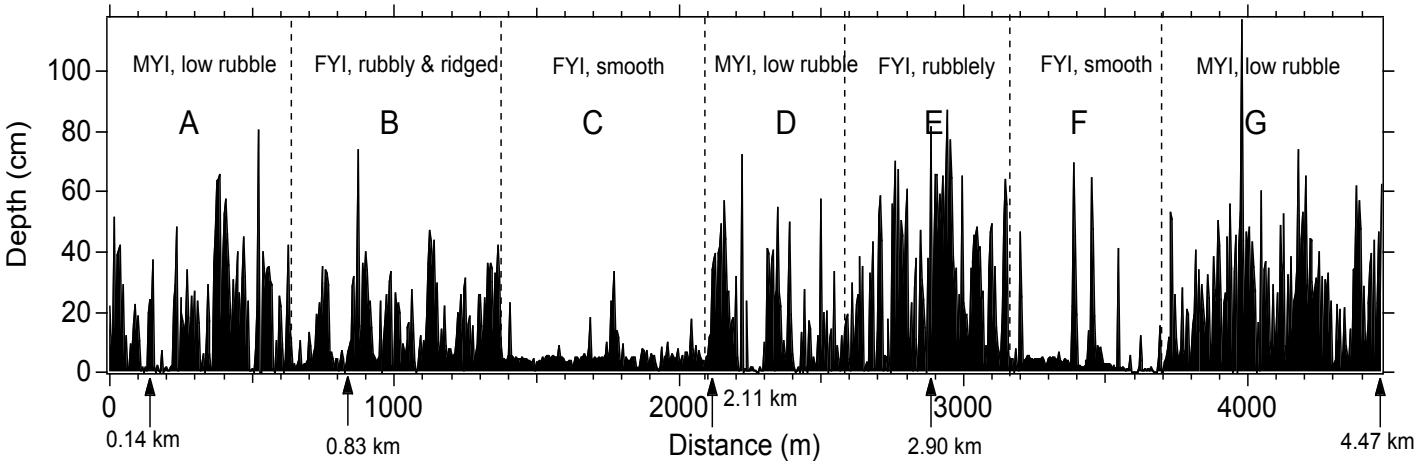

Figure 4: Snow depth profile along the main measurement line showing sectors by ice type. Arrows along x-axis denote where cross line measurements were made (Table 1). Sectors are identified by letters (A through G).

Table 1: Snow depth distribution statistics for cross measurement lines, each 0.1 km long, and sectors A through G (see Fig. 4). Mean, Std. dev., Max. and Min. have units of cm; Nugget and Sill have units of cm^2; Range is in m.

Sector	Mean	Std. Dev.	Max.	Min.	Nugget	Sill	Range	Type of Ice
2.90 km	44	19	85	3	50	320	7	MYI & FYI, large rubble
E	28	22	87	0	250	300	80	FYI, rubbly
G	26	18	117	0	220	140	100	MYI, low rubble
4.47 km	24	13	69	1	50	110	12	MYI, widely spaced rubble
0.83 km	22	17	62	0	5	335	23	FYI, rubbly
0.14 km	21	16	69	0	0	330	14	FYI low rubble, flat
A	18	17	80	0	130	200	55	MYI, low rubble
B	16	13	74	0	65	145	55	FYI, rubbly & ridged
D	15	17	72	0	180	170	120	FYI, low rubble
2.11 km	10	14	51	0	10	140	14	MYI, rounded rubble
F	7	12	70	0	0	165	26	FYI, smooth
C	6	4	34	0	8	13	47	FYI, smooth

Roughness was a better predictor than age of the ice for snow depth, with rougher ice associated with greater depths. For example, a MYI floe at 2.11 km had subdued, rounded surface topography and a snow cover that was almost as thin as that found on smooth FYI, while a MYI floe with rough, ridged ice had the deepest snow. In general, the rougher ice also exhibited a higher maximum depth. Results from semivariograms related to the structure of the depth distribution (Nugget, Sill and Range in Table 1) (Fig. 5) were less conclusive. Semivariance, which is closely related to standard deviation, tended to be higher for rougher ice, while the range (a measure of the structural length of

snow drift features, etc.) was lower. However, the results from the cross line at 0.83 km (green in Fig. 5) are not consistent with this trend and make interpretation difficult. An ANOVA using the data from the five cross lines indicates a) there is a significant difference in depth distribution between the deepest and shallowest snow packs, but b) no significant difference between the intermediate types of ice was present. Histograms (Fig. 6) for the various types of ice show that with increasing ice roughness (and snow depth) there was a decreasing probability of encountering bare or thinly covered ice, but also the gradation in properties from one type of ice to another.

.

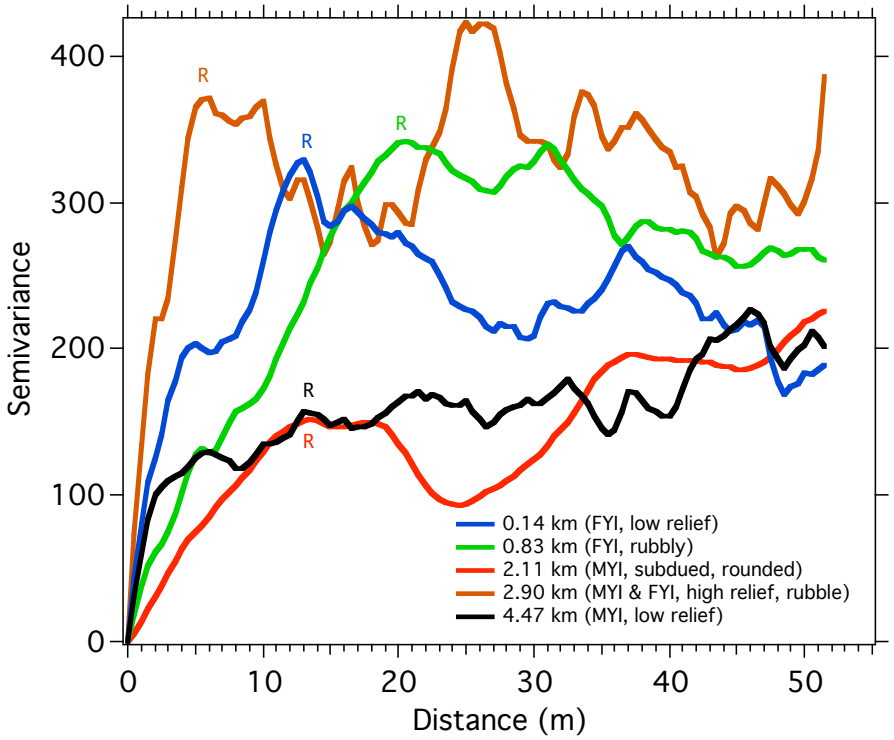

Figure 5: Semivariograms for the five cross lines at the Navy Ice Camp. The lines with the lowest ice relief had the lowest semivariance for snow depth (expected) but higher range values (marked by "R"), a measure of the structural length of the snow features.

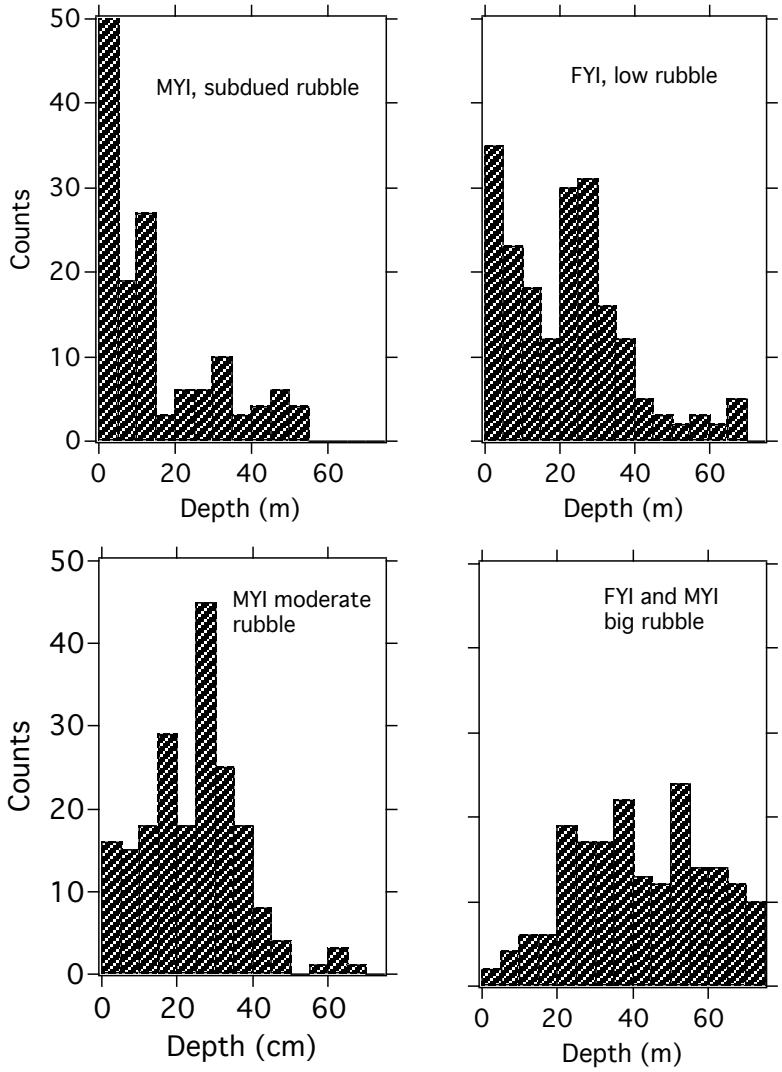

Figure 6: Histograms of snow depth for four of the 5 cross lines at the Ice Camp. MYI = multi-year ice; FYI = first year ice. Note the similarity between the distributions for FYI and MYI with subdued surface roughness.

Twenty five snow pits were dug along the main measurement line. The snow pack consisted primarily of depth hoar and wind slab (Table 2), with the later comprising 60% of the snow, though textural percentages varied markedly from place to place. About 3% of the total snow pack consisted of snow-ice, a low percentage in comparison to Antarctic sea ice, where basal flooding is common. Grain size varied over a wide range. Wind slabs consisted of equant, sub-rounded grains ranging from 0.2 to about 0.8 mm. Depth hoar grains ranged from 3 to 12 mm. These were typically hollow or skeletal prisms and pyramids with ice shell thicknesses of 0.2 to 0.5 mm. Over time on arctic sea ice wind slab metamorphoses into depth hoar, so a continuum of sizes between the two extreme types of snow always exists in the pack, and a wide range of grain sizes can be observed in virtually every snow pit.

Table 2: Snow pit texture summary, Navy Ice Camp

Location	Pit Coord	Hoar Frac.	Slab Frac.	Density (g/cm³)	SWE (cm)	No. Layers
0.14 km	0-m	0.00	1.00	0.32	11.70	2
0.14 km	25-m	0.89	0.11			4
0.14 km	50-m	0.50	0.50			4
0.14 km	75-m	0.91	0.03			6
0.14 km	100-m	0.36	0.43			8
0.83 km	0-m	0.54	0.46	0.37	8.80	6
0.83 km	25-m	0.41	0.31			7
0.83 km	50-m	0.00	1.00			1
0.83 km	75-m	0.03	0.93			4
0.83 km	100-m	0.50	0.50			2
2.11 km	0-m	0.00	0.99	0.29	2.90	2
2.11 km	25-m	0.50	0.00			2
2.11 km	50-m	0.56	0.44			2
2.11 km	75-m	0.56	0.44			2
2.11 km	100-m	0.41	0.59			7
2.9 km	0-m	0.17	0.83	0.43	25.75	7
2.9 km	25-m	0.07	0.90			3
2.9 km	50-m	0.00	0.96			4
2.9 km	75-m	0.10	0.88			5
2.9 km	100-m	0.75	0.00			4
4.47 km	0-m	0.07	0.93	0.38	22.86	7
4.47 km	25-m	0.03	0.97			3
4.47 km	50-m	0.67	0.33			2
4.47 km	75-m	0.77	0.15			4
4.47 km	100-m	0.21	0.79			2
averages:		***0.36***	***0.58***	***0.36***	***14.4***	***4***

2.2.2 Ice

Ice thickness along the main measurement line at the Ice Camp was determined by a) drilling and b) electromagnetic means (using an EM-31). Thirteen (13) bore holes (Appendix 3) were used to check the EM-31 results (634 measurements). The agreement was satisfactory. The ice ranged from 88 to 808 cm in thickness, with the former value from a smooth FYI floe, and the latter value from a pressure ridge. There was a notable correspondence between snow depth and ice thickness (Fig. 7), though because of the very irregular nature of both, the r^2 value from a linear regression between these variables was low. A histogram of the ice thickness (mean thickness: 217 cm) is shown in Figure 8.

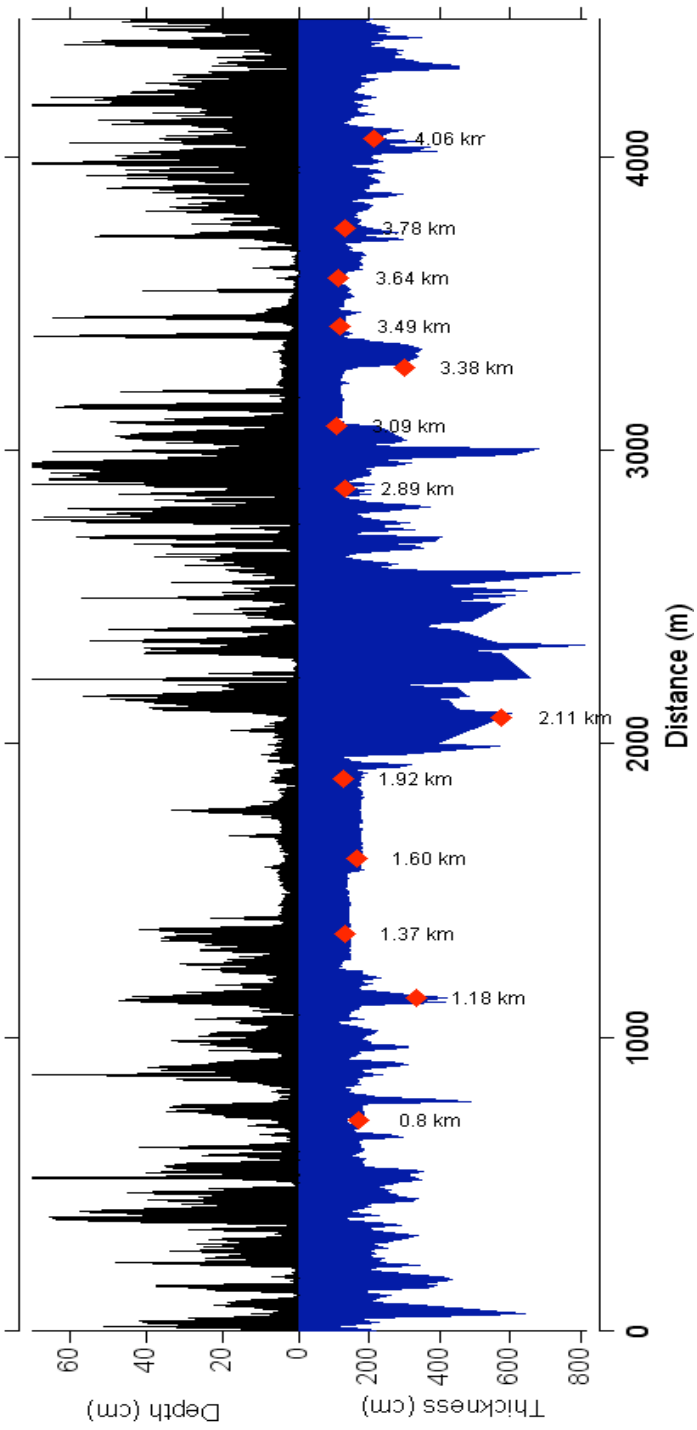

Figure 7: The main measurement line at the Navy Ice Camp, showing the ice thickness (blue) and the snow depth (black). The red diamonds are ice thicknesses determined by drilling. Note the close correspondence between the two measurements, with the hint of a downwind (toward 0 meters) shift in snow depth due to drift effects.

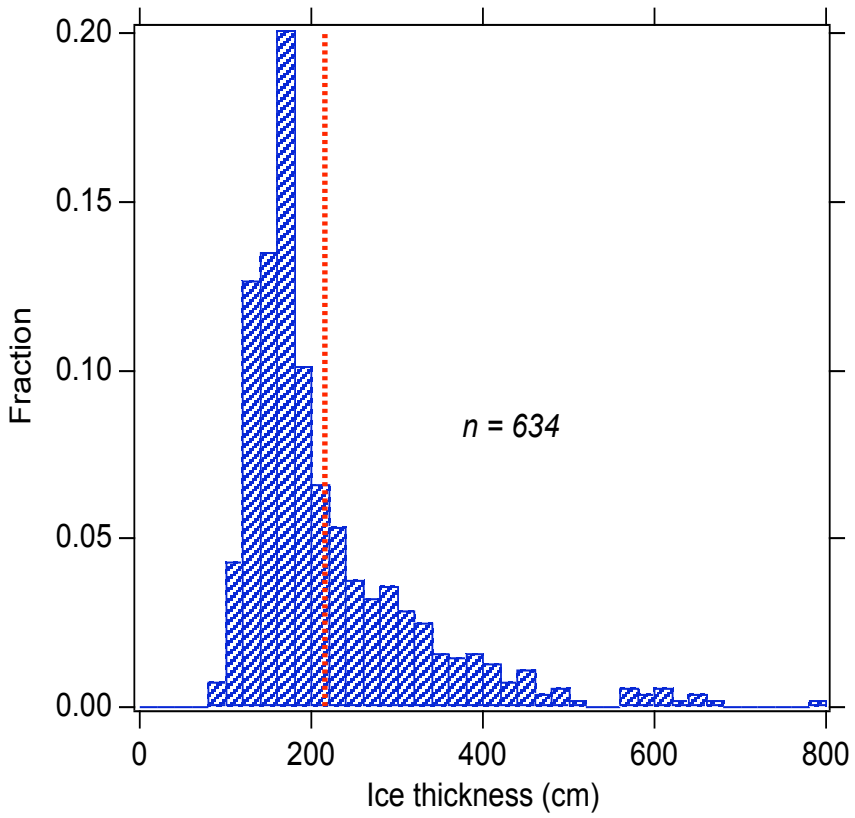

Figure 8: Histogram of ice thickness, Navy Ice Camp. The red dotted lines indicates the mean thickness.

2.2.3 Snow and Ice Temperature

During the aircraft overflight on March 19th, the temperature of the snow surface, snow base, and the ice at 10 and 20 cm depth was measured using a digital thermometer and a thermistor probe. The snow surface temperature was also measured using a radiometer. The data are presented in Appendix 4. The results (Fig. 9) indicate that the main temperature structure (a zone of cold ice in the middle of the line) was related to the thick, ridged ice in this area. There is also a suggestion that in general MYI was colder than FYI. Snow depth also controlled the temperature, particularly the snow-ice interface temperature. A regression of the interface temperature vs. depth explained 78% of the variation in this temperature at the time of the overflight (Fig. 10).

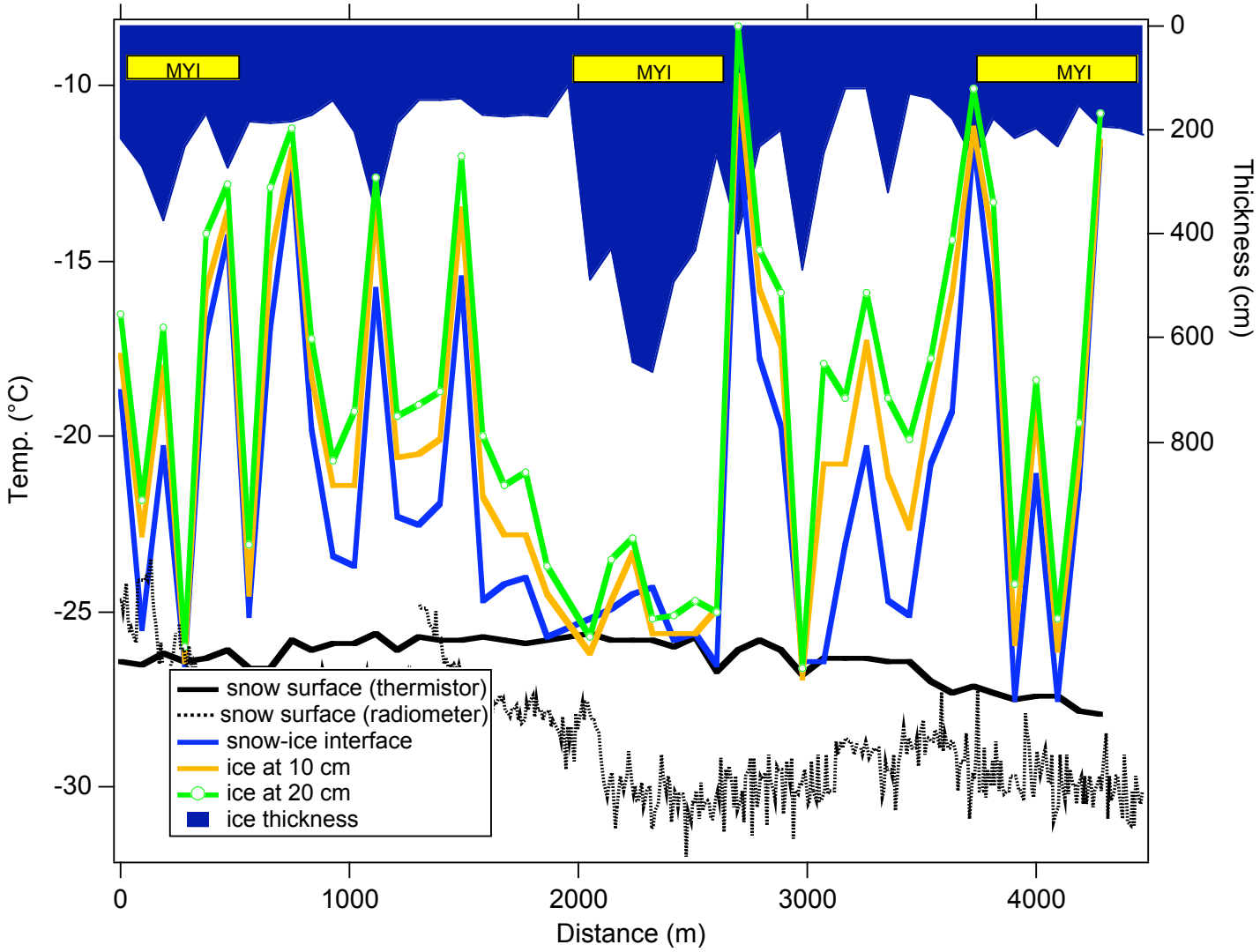

Figure 9: Snow and ice temperatures, along with the ice thickness (blue fill), and the location of MYI (yellow bars) along the main measurement line at the Navy Ice Camp. Both a thermistor and radiometer were used to measure snow surface temperatures. The former (black dotted line) indicated temperatures about 3°C lower than the latter (black solid line).

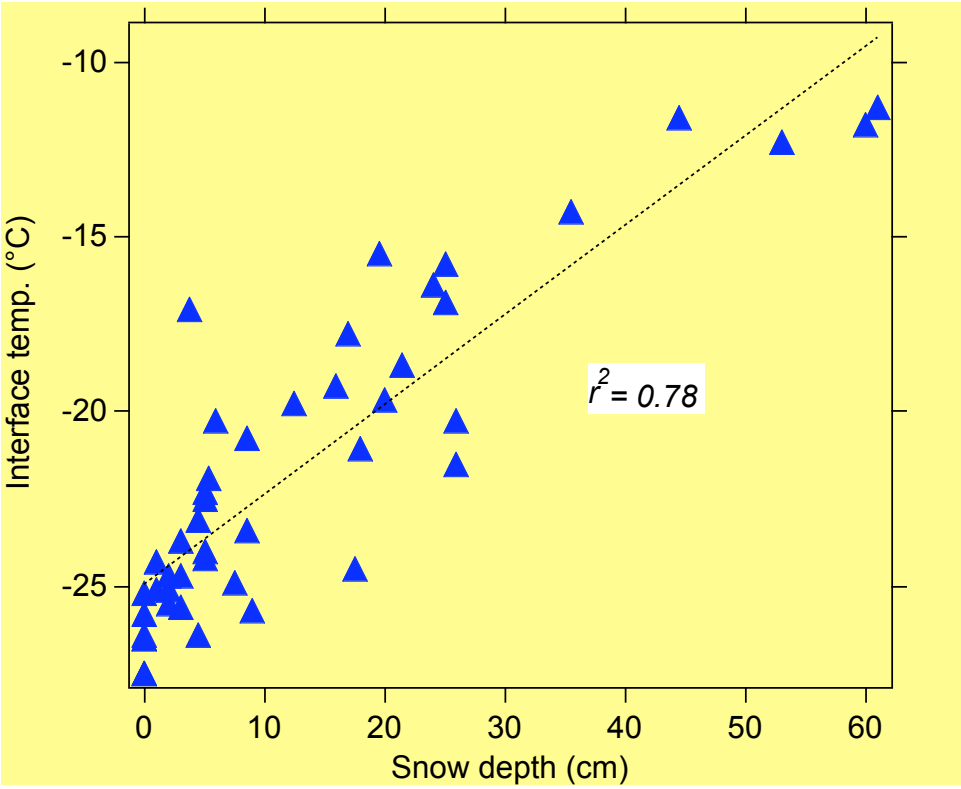

Figure 10: Snow-ice interface temperature as a function of snow depth, Navy Ice Camp.

2.3 Discussion of Navy Ice Camp Results

A wide set of snow and ice conditions were present at the Navy Ice Camp. The main and cross measurement lines sampled these nicely. The results suggest snow and ice properties varied at spatial scales ranging from hundreds to just a few meters, with homogenous areas more than a few tens of meters in extent uncommon. Because of this small-scale spatial structure, the best validation of the aircraft PSR and other sensor data will need to be done using the highest resolution products.

Loose but distinct relationships between snow depth distribution, ice type and thickness, and ice and snow temperature could be identified in the data. In general, rougher ice held deeper snow. The same ice was likely to have been deformed, therefore thicker, and consequently colder than less deformed ice nearby. In some cases, however, the effect of deeper snow (more insulation) offset the impact of thicker ice (farther distance to oceanic heat source), producing higher ice temperatures. Structural analysis (semivariograms), which in the past has revealed inter-relationships between ice roughness and snow drifting, failed to reveal any marked relationship in ice and snow characteristics, probably because the snow was quite thin at the Camp and had failed to “fill-up” to the potential snow-trapping limit of the ice, thereby reducing the potential contrast between rough and less rough ice.

As usual for arctic sea ice, snow layer characteristics varied over an extreme range. The two primary components of the snow pack, depth hoar and wind slab, have diametrically different characteristics. One is a weak, large-grained material of high insulating value. The other is a strong, dense material that is a poor insulator. Grain size between the two types of snow can vary by a factor of 30X or more. The only "well-behaved" aspects of this snow pack is that the depth hoar reliably can be found beneath the wind slab, and in most instances there are rarely more than 5 layers of snow.

A sled-mounted microwave radiometer is used to measure the brightness temperature of the sea ice on the Chukchi Sea, March 13, as in the distance the NASA P-3 Orion comes barreling down the measurement line.

3. Barrow

3.1 Barrow Field Locations

The Barrow field work was done in three areas. Area 1 was the moderately deformed ice on the Chukchi Sea. Area 2 was the smooth, undeformed ice of Elson Lagoon, and Area 3 was the heavily deformed ice of the Beaufort Sea southeast of Pt. Barrow (Fig. 11). Measurements were made in the three areas along 2 intersecting transect lines. These were marked by 3-m high black tetrahedra (visible from the air) and with lath drilled into the ice. Once marked, a swath bracketing the transect lines was photographed from a small aircraft (Cessna 185) and photo-mosaics of the lines were constructed (e.g., Fig. 12). Using the mosaics, we have been able to extrapolate our line measurements to homogeneous areas of ice, producing strip maps of several hundred meters width comparable with aerial remote sensing products.

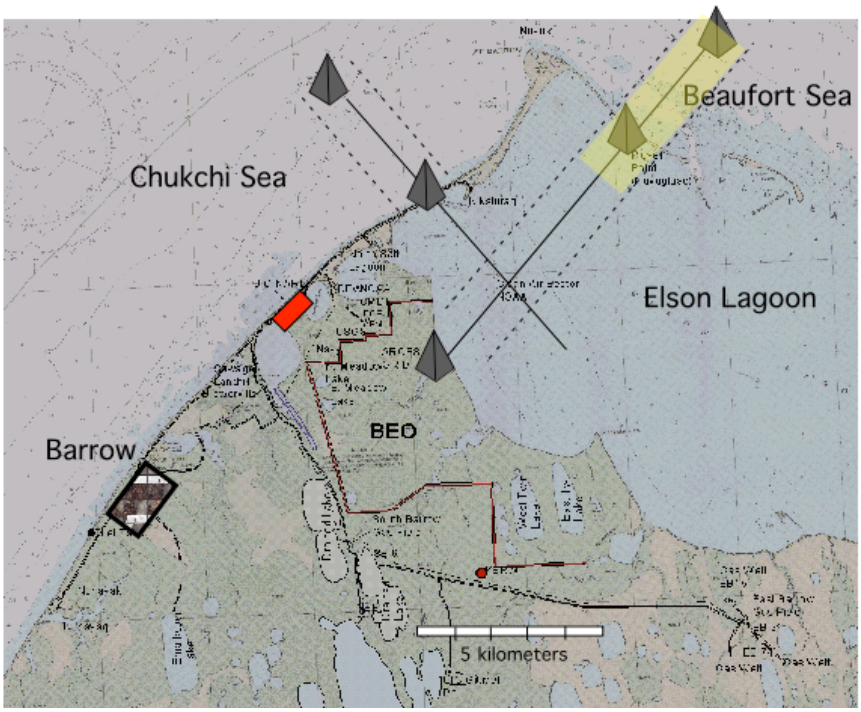

Figure 11: Barrow area map showing the Chukchi, Beaufort and Elson measurement areas and the two intersecting traverse lines, as well as the approximate swath (dashed lines) of aerial photography. The yellow area indicates the coverage of the example photo-mosaic shown in Figure 12.

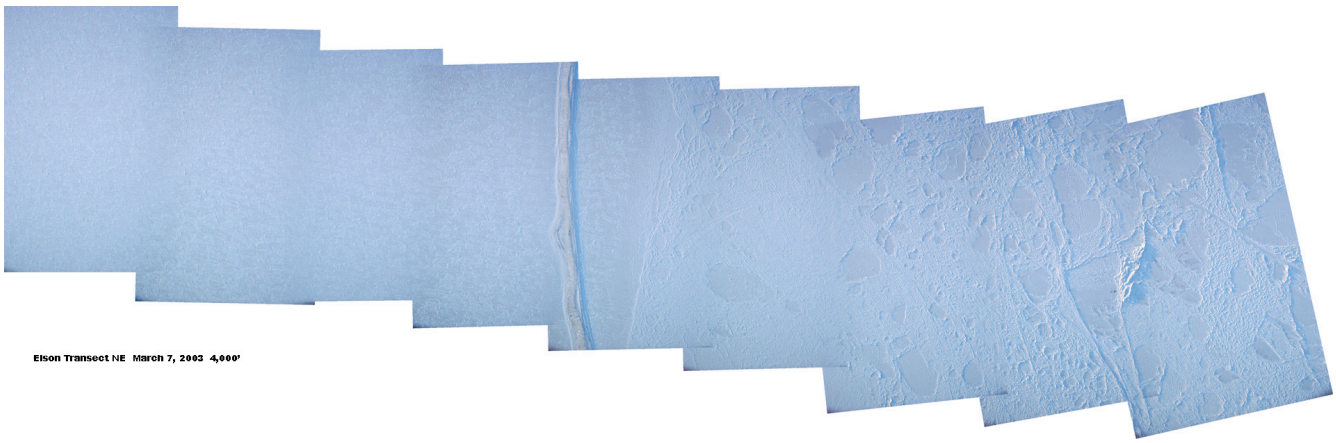

Figure 12: Aerial photo-mosaic for part of Elson Lagoon (left) and the Beaufort Sea (right) separated by the Plover Point spit.

3.2 Aircraft Overflight Locations

The NASA P-3 aircraft overflew the Barrow field area on March 13th. In order to ensure a close association between aerial remote sensing data and ground measurements the aircraft flew at its minimum altitude (about 150-m) and bracketed the two traverse lines (Fig. 11) in 9 passes. A second, higher set of passes (1200-m) were flown to ensure wide coverage. Ground observers stationed at 3 places along the lines collected notes on aircraft position during the low passes in order to aid comparison of aerial and ground data (Table 3). Because ground observers could see the black tetraheda marking the lines, these estimates of aircraft offset are accurate to about ±25 m. Because of snow and ice heterogeneity, for the most precise comparison of field and aircraft data, these offsets will need to be considered. To date, the aerial data, in particular, the PSR data, has not been released.

Table 4: Estimates of P-3 aircraft offset from the Barrow on-ice traverse lines, March 13, 2003

Time (AST)	Line	Flight Direction	Offset Direction	Distance (m)
10:45	Elson_Beaufort	NE	NW	200
?	Elson_Beaufort	SW	--	0
?	Chukchi	NW	?	?
?	Chukchi	SE	SW	100
11:09	Elson_Beaufort	NE	NW	100
11:16	Chukchi	SE	SW	100
11:26	Chukchi	NW	SW	250

11:34	Elson_Beaufort	NE	NW	50
11:46	Elson_Beaufort	SW	NW	150
11:52	Chukchi	NW	SW	50
12:03	Chukchi	SE	SW	150
12:10	Elson_Beaufort	NE	NW	100
12:22	Elson_Beaufort	SW	SE	50
12:28	Chukchi	NW	--	0
12:38	Chukchi	SE	--	0
12:44	Elson_Beaufort	NE	SE	25
12:53	Elson_Beaufort	SW	SE	100
13:00	Chukchi	?	NE	50
13:09	Elson_Beaufort	SW	SE	25

The on-ice measurements consisted of:

- Meteorological data and in-situ snow and ice temperatures (7 locations).
- Snow depth.
- Snow stratigraphy, density and grain size.
- Ice thickness (from bore holes and using an EM-31).
- Ice cores for physical properties.
- Snow and ice temperature.
- Snow “skin” temperature (using a KT-19).
- Brightness temperature, 81 GHz.

3.2 Results-Barrow Area

3. 2.1 Snow

The snow distribution for the Chukchi Sea is shown in Figure 13 against a background of the aerial photo-mosaic for that line taken March 7th. Snow depths were measured every 3 meters along the main line (*n*= 1340), and every 0.5 m on six 100-m lines that were located adjacent to the main line (*n* = 1206). Similar data were collected on Elson Lagoon, on the Beaufort Sea (Appendix 5), and at the Navy Ice Camp (Appendices 1 and 2).

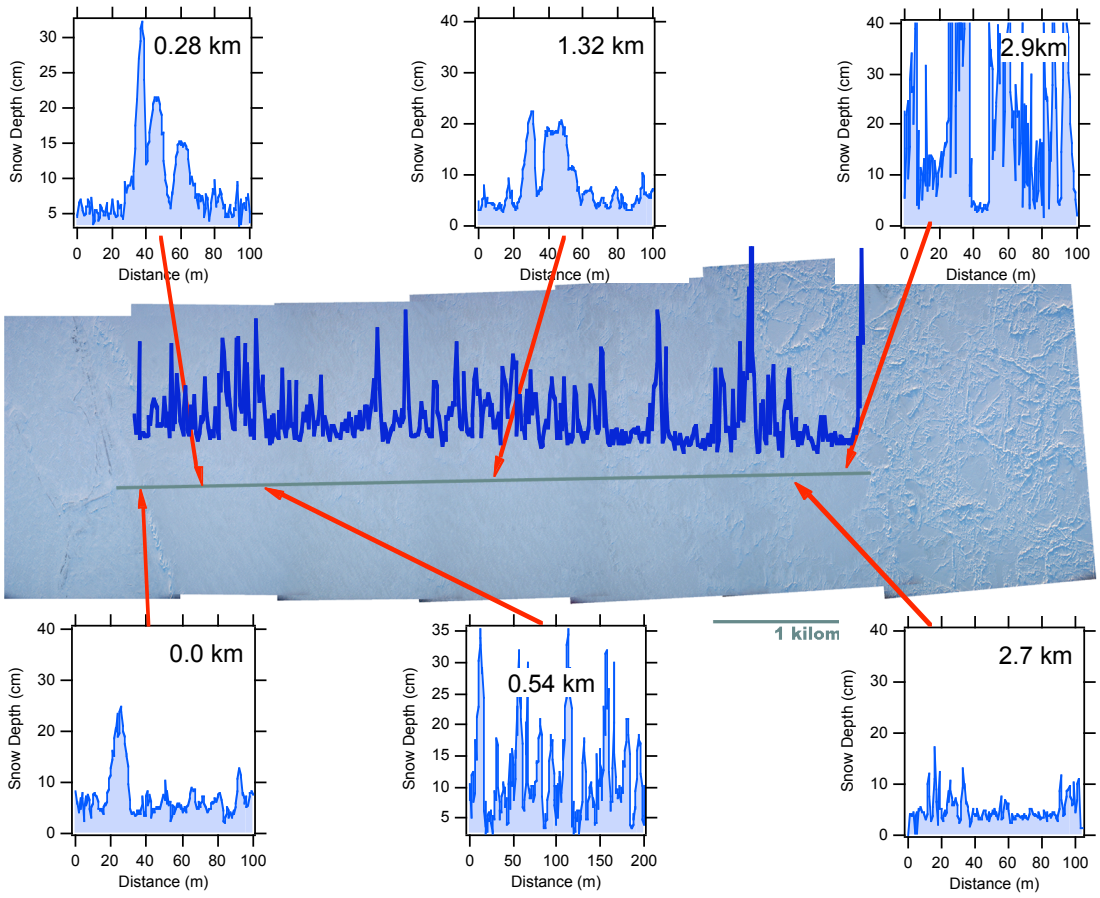

Figure 13: Snow depth distribution along the Chukchi transect line, with data from six 100-m lines shown as insets. The transect runs from the shore (left) to an area of rubble ice and pressure ridging (right) beyond which it was difficult to travel and make measurements. The heavy blue profile superimposed on the photo-mosaic has a point spacing of 3 meters. The six inset profiles have spacing of 0.5 m.

We have compared (Fig. 14) the depth distribution histograms from the three Barrow areas with the results from the Navy Ice Camp. The Navy Ice Camp and the Beaufort Sea had very similar distributions, despite the fact that the former had an ice cover consisting of both FYI and MYI, while the latter had only FYI. These two sites also shared in common a) similar ice roughness (they were both rough), and b) a sizeable fraction of bare, or nearly bare ice floes, perhaps because new ice production was more continuous in these more dynamic areas. This similarity is emphasized even more when semivariograms for all three Barrow areas, plus the Navy Ice Camp are compared (Fig. 15).

Figure 14: Depth distribution histograms for Elson, Navy Ice Camp, Beaufort and Chukchi field areas. The vertical red dashed line is the local mean depth in each area. The black dotted line on the Beaufort panel is

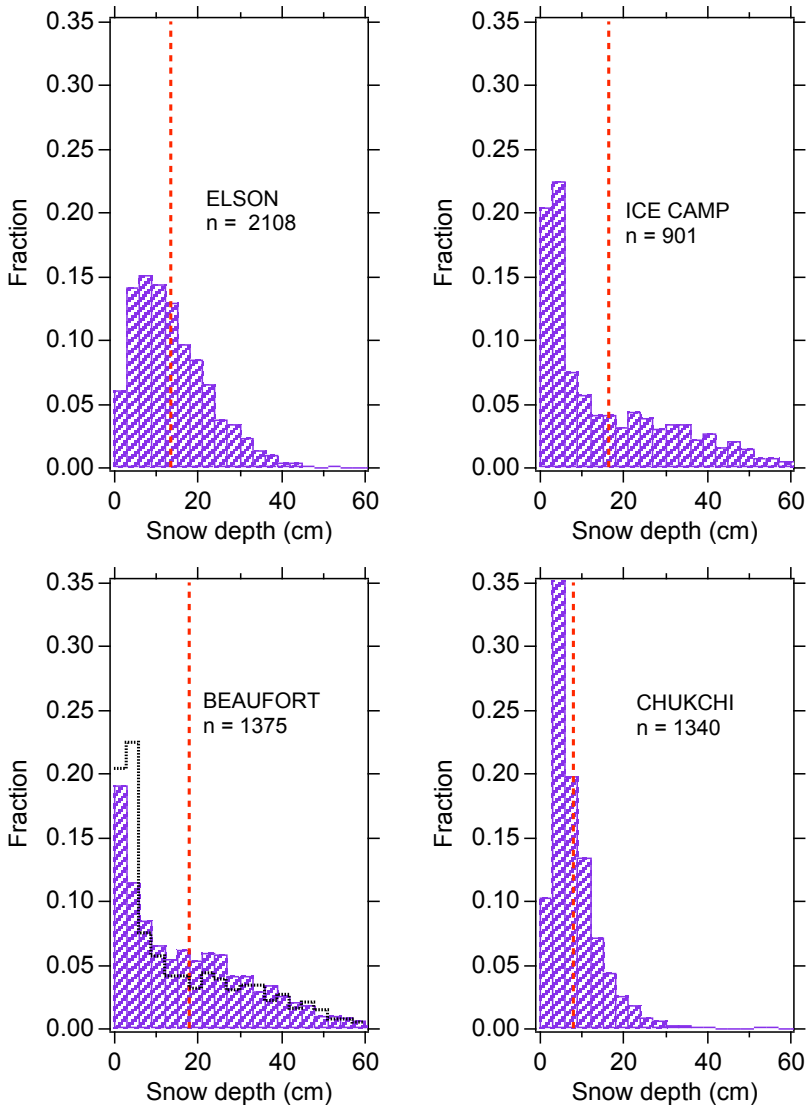

the distribution histogram for the Ice Camp.

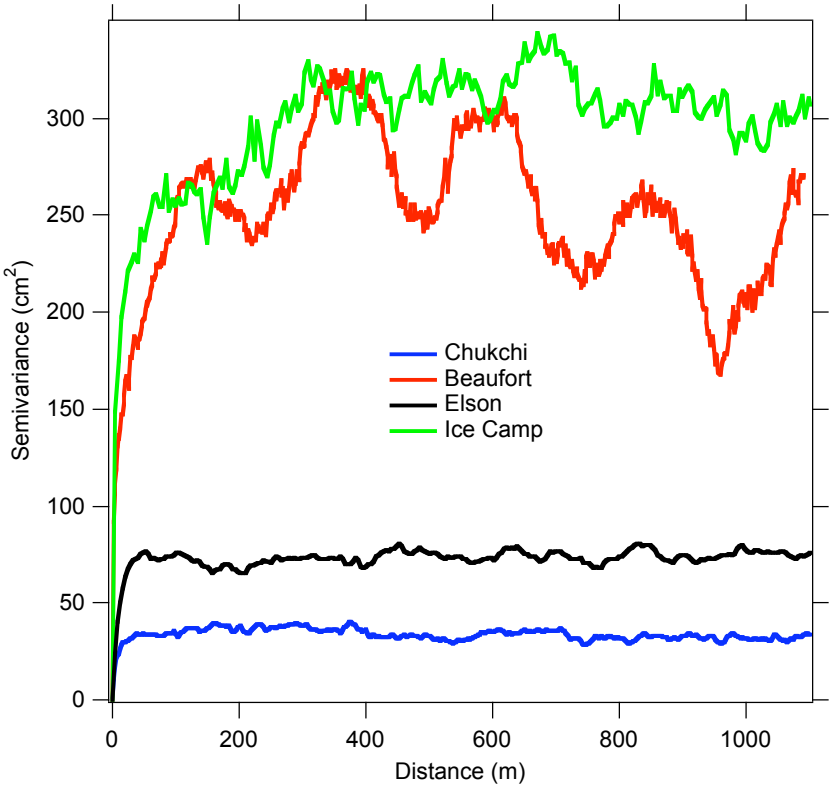

Figure 15: Semivariograms of the snow depth at the three Barrow areas, as well as at the Navy Ice Camp in the Beaufort Sea. The Ice Camp and the Beaufort Sea near Pt. Barrow had similar variograms, indicating a similar roughness (semivariance), and a similar structural length scale for snow depth (> 200 m) imparted to the snow by both the ice roughness and wind drifting. In contrast, Elson Lagoon and the Chukchi Sea had smoother variations in depth with much shorter structural lengths.

In the Elson Lagoon area and Beaufort areas, we measured snow and ice surface roughness using a laser ranging system (Fig. 16a). The results are similar to results we have obtained before from the Beaufort Sea during project SHEBA and from ice floes in the Antarctic. The ice surface is rougher on a small spatial scale than the snow surface. The snow tends to smooth out ice roughness elements, leading to a more gently undulating surface, though one with the same amount of vertical relief. This smoothing effect is evident when comparing semivariograms for the snow surface and snow base (Fig. 16b), where the semivariance of both curves is about the same, but the range for the snow surface is more than 20 m, while it is less than 3 m for the ice. This transition from a rough-on-a-fine scale ice surface to an undulating snow surface is consistent with our observations of whaleback-shaped snow drifts with 10 to 40-m length scales in many areas.

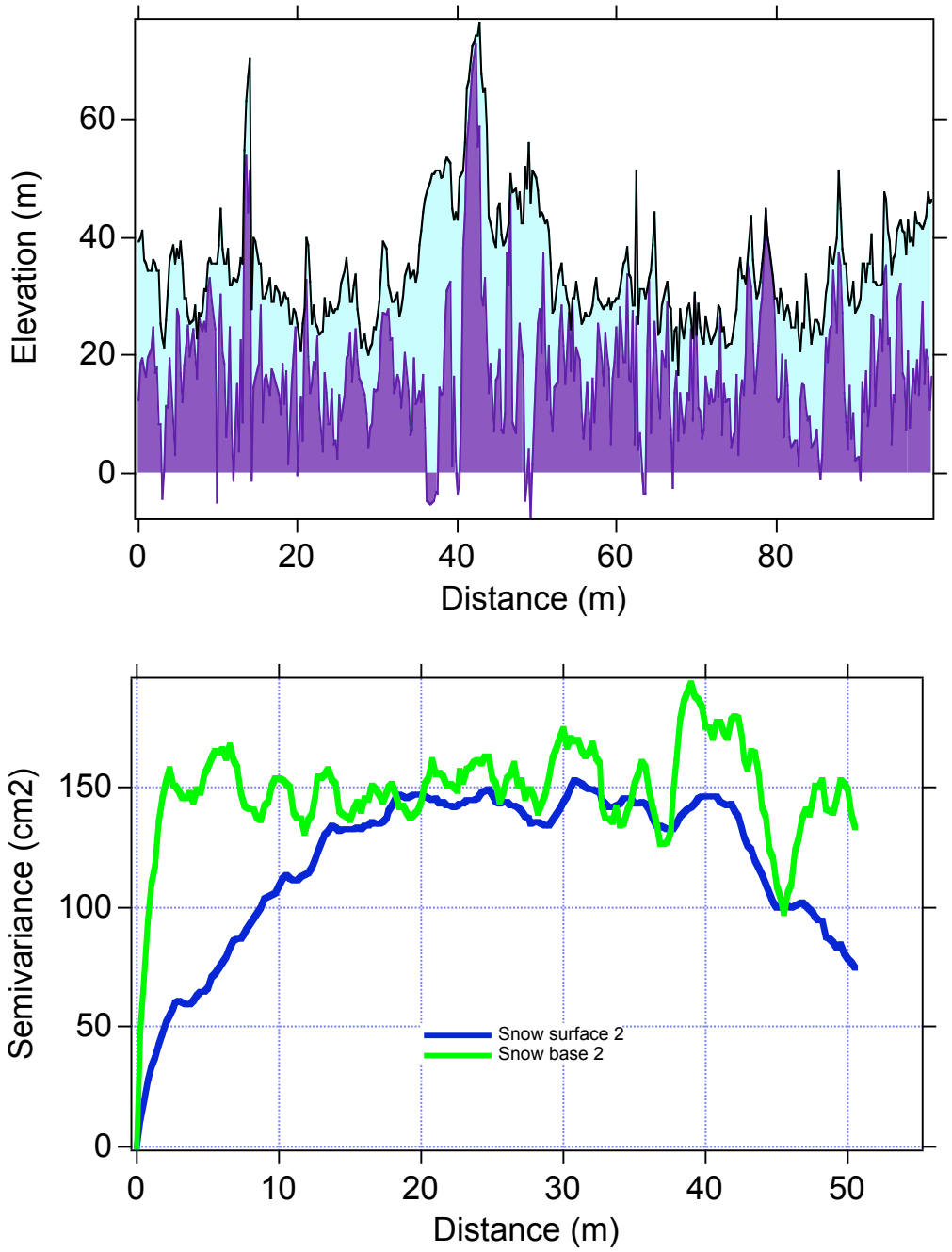

Figure 16a (top): A cross section of the snow (light blue) and ice (maroon) surfaces on Elson Lagoon. Figure 16b (bottom): Semivariograms for the surfaces shown in Figure 16a. The range, or structural length scale is the distance at which the semivariance plateaus at a maximum value.

We investigated whether the orientation of the measurement lines produced a bias in the depth distribution data by comparing the results from the Chukchi Main line to

results from a line that ran perpendicular to it (Chukchi Cross Line). The cross line was 1.5 km long, compared to 2.9 km for the Main line. Mean depths (8.1 vs. 7.6 cm, Main vs. Cross) and standard deviations (6.0 vs. 5.5 cm) were within 7% of each other, and the distribution histograms a were nearly identical (Fig. 17), suggesting little or bias due to line orientation.

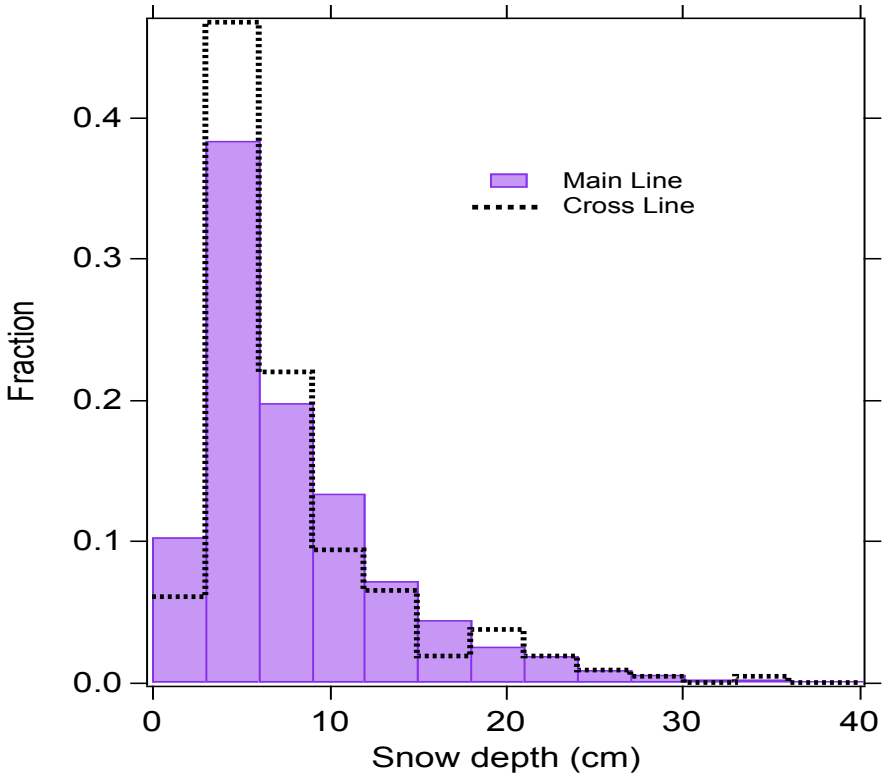

Figure 17: Snow depth distribution for the Chukchi Main and Cross lines.

Snow stratigraphy , density and grain size were investigated in 95 snow pits (Appendix 6) distributed uniformly across the three Barrow field areas. The results indicate that on the rough ice of the Beaufort Sea the snow pack consisted of more and thicker layers of snow than the pack on the Chukchi Sea and Elson Lagoon, but that these layers were 12 to 22% less dense than their thinner counterparts in the other areas. There was 2 to 3 times as much snow water equivalent on the ice of the Beaufort Sea, suggesting that by trapping the snow better than the ice in the other locations, losses due to sublimation (or transport into open leads) was reduced. The texture in all three locations was, by and large, the same: about half wind slab and about half depth hoar, with minor amounts of other types of snow. As before, data from the Beaufort Sea matched most closely the data from the ice camp (Table 5). Snow grain sizes were also similar to those at the Navy Ice Camp.

Table 5: Snow texture and stratigraphic statistics for the three areas near Barrow and for the Navy Ice Camp (see also Table 2 and Appendix 6)

	Hoar Frac.	Slab Frac.	Density (g/cm^3)	SWE (cm)	No. Layers
Navy Ice Camp	0.36	0.58	0.36	14.4	4
Beaufort Sea	0.48	0.35	0.28	11.8	5
Elson Lagoon	0.51	0.40	0.36	6.1	4
Chukchi Sea	0.44	0.51	0.32	2.8	2

3. 2.2 Ice

Sea ice thickness was measured near Barrow in the same way as at the Navy Ice Camp, using the EM-31, and checking/calibrating the results using drill hole thicknesses. Based on 14 borehole-to-EM-31 comparisons, a correction of –12 cm was applied to the Barrow data.

Ice thickness for the heavily deformed Beaufort Sea was closely correlated with snow depth (Fig. 18), with rough, deformed ice holding markedly deeper snow. Aerial photo-mosaics could be used to identify undeformed and deformed areas, and in this way, used to predict in a general sense both the ice thickness and the snow depth. In other areas around Barrow the relationship between thickness and depth was not as well developed, but still recognizable.

The ice thickness distribution at the three areas near Barrow and at the Ice Camp are shown in Figure 19. Again, the data suggest a close affinity between the results for the Beaufort Sea and the Ice Camp. The ice of the Chukchi Sea had a narrow distribution centered a mean value of 128 cm. The ice in this area was swept away in November, 2003 and then all of it reformed probably by congelation growth, accounting for the low mean value and the limited range in thickness. The Beaufort and Ice Camp sites had long “tails” of thick ice in their distributions due to keel formation under ridges.

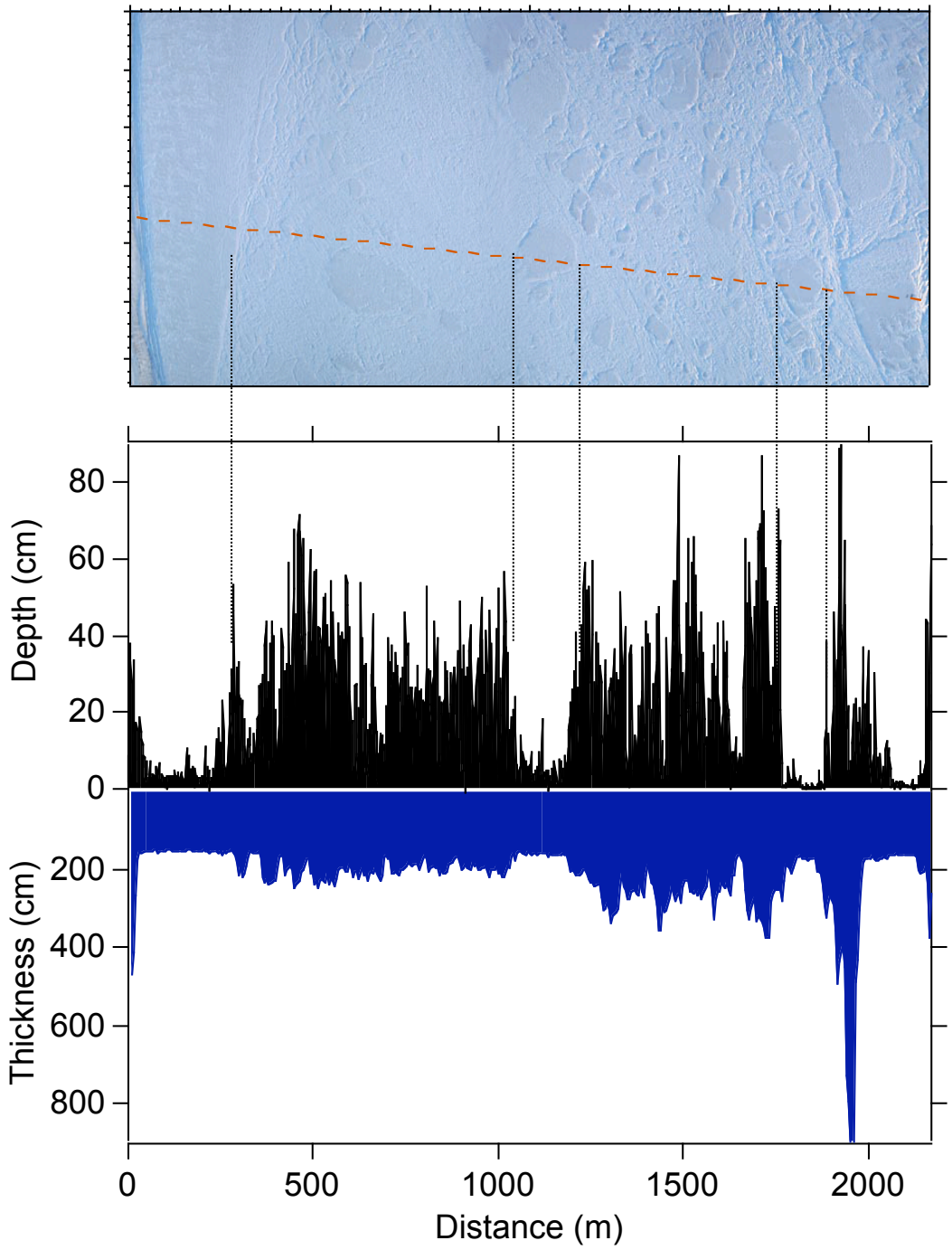

18: Ice thickness and snow depth along the main transect line, Beaufort Sea, showing a striking correlation between the two variables. Undeformed floes (with thin ice and snow) surrounded by deformed ice and rubble fields can be seen in the photo-mosaic (top panel).

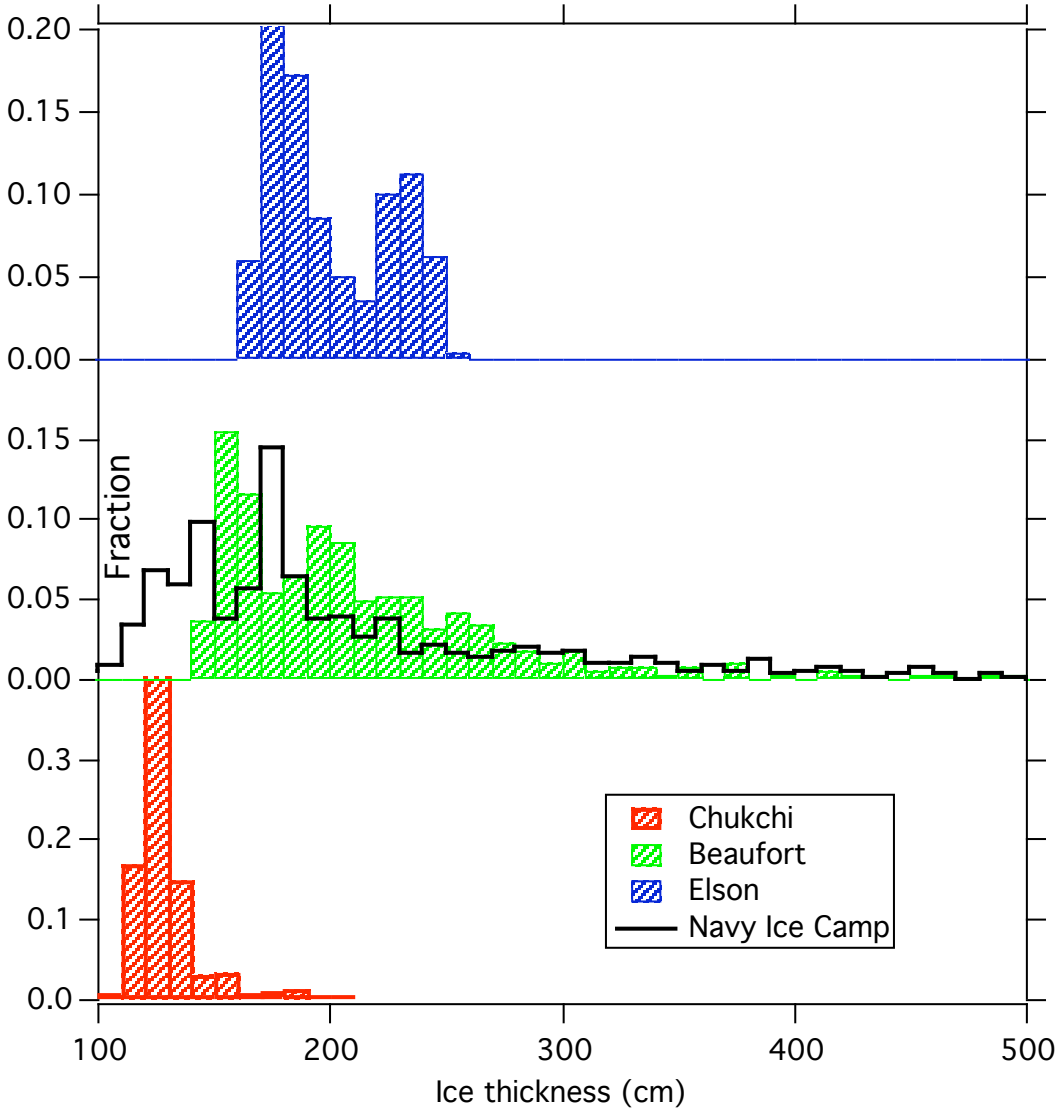

Figure 19: Ice thickness distribution histograms for the three areas near Barrow and the Navy ice camp.

3.2.3. Snow and Ice Temperatures

During the March 13 overflight, the temperature of the snow and the ice were measured along the transect lines using digital thermometers and a KT-19 radiometer. The overflights took more than 3 hours, so there was a temporal drift to the snow surface temperature. In addition, there seemed to be some ice/snow controls on the surface temperature that led to "fixed" structures in temperature, as seen in Figure 20.

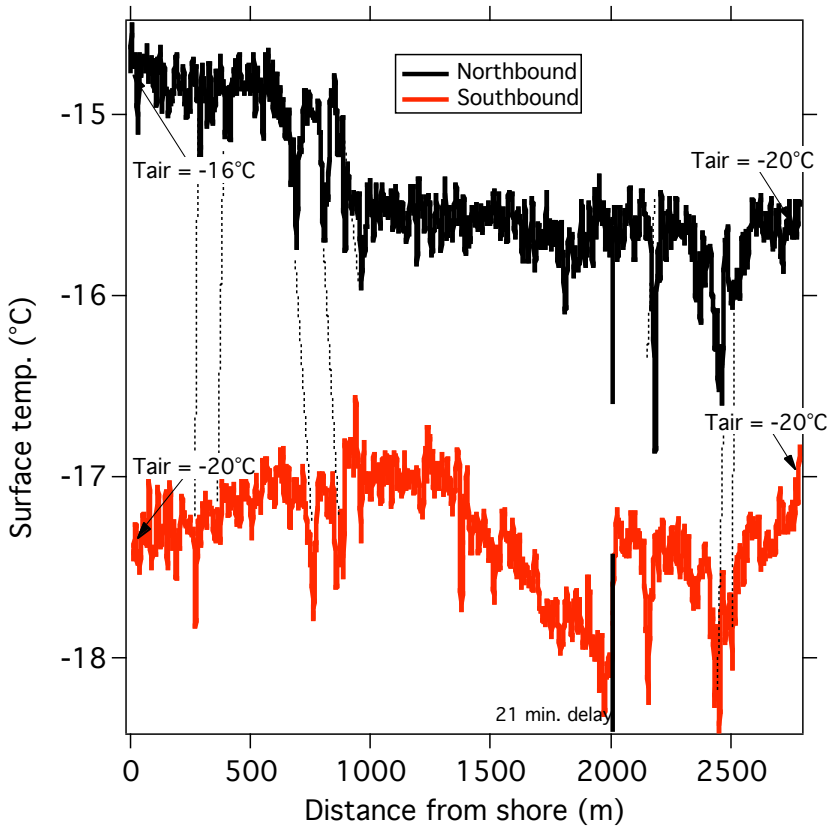

Figure 20: Surface temperature of the Chukchi line on March 13 during the NASA P-3 overflight. The run out (black) and back (red) took substantial time and the surface temperature changed during a long pause between runs. Vertical dashed lines indicate structures that persisted on the second run, despite the temporal shift in temperature.

We have examined the relationship between the snow-ice interface temperature, the ice temperature at 10 cm depth, and the snow depth in the three Barrow field areas (Fig. 21). The overflights took place after the temperature had been dropping for about a day (from –20 to –26°C). Both interface and ice temperatures were linearly related to the snow depth, but the slopes differed from one area to another, with the Beaufort Sea having the lowest slope, and the Chukchi Sea having the highest slope. In the most general way, this slope is measure of a) the insulation value of the snow, and b) the proximity of ocean heat flow. Steeper slopes imply better insulating snow and thinner ice. This may explain why the Chukchi Sea, with its thin ice, had the highest slope. The Barrow results are comparable to the Navy Ice Camp results (Fig. 10).

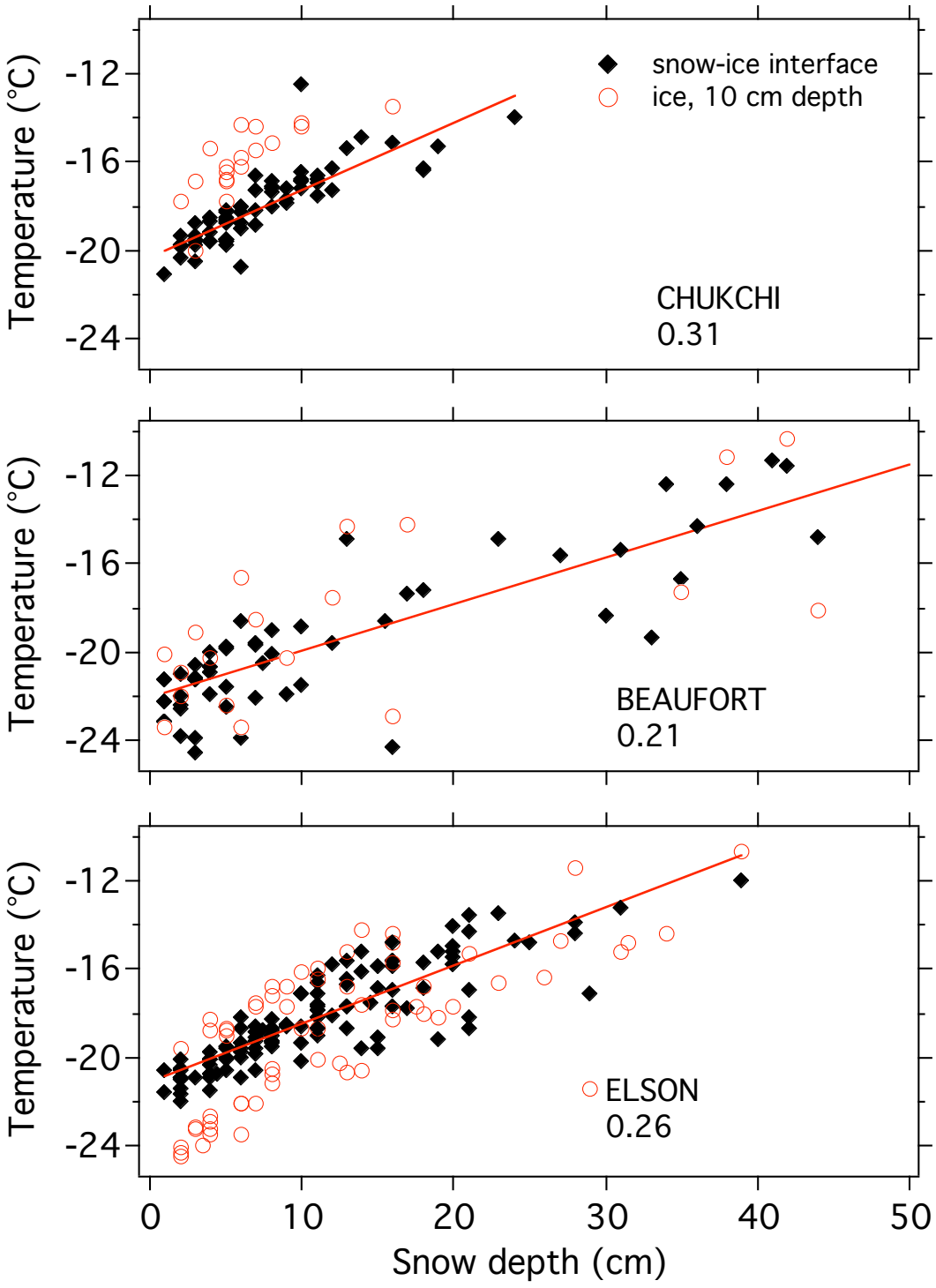

Figure 21: Snow-ice interface temperatures, and 10-cm deoth ice temperatures as a function of local snow depth for the three Barrow field areas. The number beneath the area name is the slope of the best fit line to interface temperature.

4. Continuing Work

Two data sets were not available at the time of writing this report:

- Ice cores: they are being analyzed for salinity, structure and brine pocket distribution
- Brightness temperature: Dr. Tom Grenfell of the University of Washington is applying the calibrations to these data which were collected during the NASA P-3 overflight on March 13th. The data are best for the Chukchi line, and marginal for the Elson-Beaufort line, where equipment malfunction prevented collection of a complete record.

Data from the P-3 aircraft are now available from March 19th, but the data for the Barrow overflight on March 13th have not yet been processed. We are currently in the process of comparing the on-ice conditions at the Navy Ice Camp with the PSR data at highest resolution. We are also using P-3 on-board aerial photographs and MODIS imagery to create a set of field maps of the Ice Camp area on which we can more accurately place and extrapolate the on-ice data. As this work progresses, we will be testing, then revising as needed, the algorithms for snow on ice for the AMSR-E.

5. Conclusions

The data collected during the AMSR-E calibration /validation campaign near and off-shore of Barrow, Alaska are extensive and cover most aspects of the snow and ice environment. Samples of these data have been presented above, and the data set provides an excellent "legacy" in the form of a general description of what the ice and snow conditions are like for arctic sea ice. In addition, as the aircraft and satellite data become available, the field data should provide an excellent set against which existing retrieval algorithms can be tested.

The data reinforce a well known fact: the snow and ice environment of arctic sea ice is extremely heterogeneous. This heterogeneity extends from ice thickness and snow depth to physical temperature, grain size, snow water equivalent and roughness. In many cases, the spatial scale of the variability is less than 10-m, and only for a few attributes does the scale extend to hundreds of meters (e.g., note the limited range in the various semivariograms presented in this report). One impact from this heterogeneity is that all pixels, satellite or aircraft, are "mixed". The fact that meaningful retrievals can be made from the remote sensing data implies that (fortunately), properties related to the remote sensing tend to aggregate around mean values.

One surprising finding from the field data was that the snow and ice conditions in the Beaufort Sea, just a few kilometers off of the land, were similar to the conditions at the Navy Ice Camp, hundreds of kilometers off-shore. This similarity existed, despite the fact that the near-shore Beuafort ice was FYI, while the off-shore Beuafort ice was mixed MYI and FYI. We attribute this similarity to the fact that roughness, not age of the ice, was the controlling variable, with the degree of deformation the critical

factor. Thus, the near- and off-shore Beaufort ice had similar roughness, this led to similar snow-holding capacity, similar temperature conditions and so on. An implication of this finding is that it is reasonable to conduct calibration/validation campaigns near Barrow, where the costs are considerably less than those incurred conducting similar tests well off-shore.